Thin Solid Films 518 (2010) 6168–6173

Contents lists available at ScienceDirect

Thin Solid Films

journal homepage: www.elsevier.com/locate/tsf

Flexible organic thin-film transistors using single-walled carbon nanotubes as an activated channel

Jae-Hong Kwon [a], Sang-Il Shin [b], Myung-Ho Chung [b], Ki-Young Dong [b], James Jungho Pak [c], Byeong-Kwon Ju [c,*]

[a] SRAM & Design Group, Foundry Business Team, System LSI Division, Samsung Electronics Co. Ltd., Nongseo-Dong, Giheung-Gu, Yongin-City, Gyeonggi-Do, 446-711, Republic of Korea
[b] Display and Nanosystem Laboratory, College of Engineering, Korea University, Anam-Dong, Seongbuk-Gu, Seoul 136-713, Republic of Korea
[c] School of Electrical Engineering, College of Engineering, Korea University, Anam-Dong, Seongbuk-Gu, Seoul 136-713, Republic of Korea

ARTICLE INFO

Available online 31 May 2010

Keywords:
Flexible organic thin-film transistors
Single-walled carbon nanotubes
Pentacene
Cross-linked poly-4-vinylphenol
Polyethersulphone

ABSTRACT

We report on the fabrication of organic thin-film transistors (OTFTs) with a spun cross linked poly-4-vinylphenol (PVP) dielectric on a polyethersulphone (PES) flexible substrate. To improve the electrical performance of OTFTs, we employed a random single-walled carbon nanotubes (SWNTs) network as a carrier transfer underlay without sacrificing the flexibility of the TFTs. The random SWNTs showed that they can act as a semiconducting channel and conduction path to shorten the channel length in our TFTs. The flexible thin-film transistors (TFTs) with a random SWNTs/pentacene bilayer as an active channel exhibited an improved saturation field effect mobility (μ_{sat}) of 2.6×10^{-1} cm^2/Vs compared to that of TFTs without the SWNTs underlay, while creating only a minor reduction of the current on/off ratio.

1. Introduction

Organic thin-film transistors (OTFTs) are expected to be a promising device for organic electronics including, flexible displays such as organic light emitting diodes (OLEDs), electronic paper, radio frequency identification tags (RFIDs), sensors, solar cells, and smart cards [1,2]. The device performance of OTFTs based on pentacene organic semiconductor (OSC) is comparable to that of hydrogenated amorphous silicon thin-film transistors (a-Si:H TFTs). Existing research trends of OTFTs are in the direction of developing novel OSCs to increase the mobility and high capacitance gate dielectric to reduce the operating voltage [3–6]. Many researchers have been attracted by their compatibility with flexible substrates and the possibility of low-cost fabrication at room-temperature. Moreover, the TFTs that are based on flexible substrates have received considerable interest in the recent year because, flexible electronics have been proposed for a number of emerging applications such as flexible active matrix displays and memories. In order to fully utilize these advantages, developments of an improved active channel and a suitable gate dielectric without sacrificing the flexibility of the TFTs are required.

To improve the active channel of TFTs with an OSC, the single-walled carbon nanotubes (SWNTs) are a promising candidate. The SWNTs have been of great interest due to remarkable structural and electrical properties [7]. The random SWNTs network is easily formed by spin, drop, and spray coating methods. While the semiconducting SWNTs generally show unipolar *p*-type behavior in an ambient environment [8,9], the random SWNTs network has shown that it can act as a semiconducting channel and conduction path in the TFTs device, due to dominant semiconductor and minimal density metallic tubes [10,11]. Consequently, it would be better to use the random SWNTs network as a modification layer that ameliorates the electrical characteristics of the OTFTs on flexible substrates. In addition, the use of an organic gate dielectric is likely to be an important element of flexible electronics. Among the various organic gate dielectrics, poly-4-vinylphenol (PVP) is attracting considerable attention [12–14]. The cross-linked PVP dielectric might have only a minimal density of OH groups and internal impurities, so the remnant dipole effects become minimized and interfacial charge carrier traps could be effectively decreased.

In this paper, we report on the fabrication and the characterization of flexible TFTs with a random SWNTs/pentacene bilayer as an active channel, cross-linked PVP as a gate dielectric, and polyethersulphone (PES) as a flexible substrate. We achieved a narrow band gap semiconductor and a minimal density metallic component in the random SWNTs network, and these characteristics play an important role in enhancing the transconductance of our flexible TFTs, while they caused a slight degradation of switching characteristics because of the relatively high off-state current (I_{off}). This indicates that the nanotubes underlay reduces the channel length in flexible pentacene TFTs, so it improves the mobility without a significant loss in the on/off current ratio.

* Corresponding author. Tel.: +82 2 3290 3237; fax: +82 2 3290 3791.
E-mail address: bkju@korea.ac.kr (B.-K. Ju).
URL: http://diana.korea.ac.kr (B.-K. Ju).

0040-6090/$ – see front matter © 2010 Elsevier B.V. All rights reserved.
doi:10.1016/j.tsf.2010.04.052

2. Experimental

2.1. Device fabrication

Fig. 1(a) shows a schematic of TFTs with the pentacene/random SWNTs bilayer, and Fig. 1(b) shows an optical image of a bend in our flexible and semitransparent TFTs. The 150 nm thick indium–tin oxide (ITO) sputtered on a 100 μm thick PES was used as a bottom gate electrode and flexible substrate, respectively.

To prepare the PVP (Sigma-Aldrich, Mw ~20,000) dielectric solution, the PVP powder was mixed with propylene glycol monomethyl ether acetate (PGMEA) with 13 wt.%. We added a cross-linking agent, poly melamine-co-formaldehyde methylated (Sigma-Aldrich, Mwn ~511) into the PVP solution with a ratio of 1:20. The PVP solution was coated on the PES substrate, and a curing process was successively conducted at 200 °C for 10 min on a hot plate to enforce the cross-linking of the polymer. The final thickness of the PVP dielectric measured by a surface profiler (Dektak 3030 profilometer) was 450 nm.

The SWNTs powder (Iljin Nanotech Co., Ltd., ~90% purity) synthesized by the arc discharge process had an average diameter of 1.2 nm and length of 5~20 μm. To prepare the suspension of SWNTs, the powders were dispersed in a surfactant solution containing of 0.6 wt.% aqueous sodium dodecyl sulfate (SDS). After mixing, the suspension was sonicated for 2 h using a probe sonicator, and then it was centrifuged at 15,000 rpm for 4 h. The final suspension approached the SWNTs concentration of 30 mg/l [11,15]. Prior to evaporation of the pentacene layer, the random SWNTs underlay was deposited on the PVP dielectric film by using the spin-coating method.

The 70 nm thick pentacene (Sigma-Aldrich, ~99% purity) overlay on the random SWNTs underlay was evaporated at a deposition rate of 0.3 Å/s under a base pressure of 1×10^{-6} Torr. The 250 nm thick Au source and drain electrodes were deposited on the surface of the pentacene film to obtain a top-contact structure through a shadow mask by a thermal evaporator (DOV Co., Ltd). The channel width and length were 1000 μm and 100 μm, respectively.

2.2. Measurements

An atomic force microscope (AFM, PSIA XE-100) was used to characterize the surface roughness of the spun PVP dielectric and to observe the surface morphology of the thermally deposited pentacene film onto the random SWNTs underlay and onto the PVP dielectric, respectively. The structural property of the pentacene film was characterized by X-ray diffraction (XRD, Rigaku diffraction D/max 2200 V) spectroscopy in the symmetric reflection coupled θ–2θ arrangement with CuKα_1 radiation ($\lambda_{K\alpha1}=1.5046$ Å) X-ray source. The surface energy of the PVP dielectric was examined by contact angles using distilled water and ethylene glycol (Sigma-Aldrich, 99% purity). The contact angle measurements of the PVP dielectric film were performed by a contact anglometer (Phoenix 450) with a drop volume of 50 μl. The electrical characteristics were measured in order to evaluate the electrical performance of the TFTs using the semiconductor characterization system (Keithley SCS 4200) in a dark box.

3. Results and discussion

3.1. Characterization of the dielectric film

Fig. 2 shows AFM images and the contact angles of the PVP dielectric. The surface roughness (root mean square) of the PVP dielectric was 0.44 nm. To calibrate the surface energy of the PVP dielectric, we measured the contact angles using deionized water and ethylene glycol as a reference liquid along with the following equation [16], $(1+\cos\theta)\gamma_r = 2(\gamma_s^p\gamma_r^p)^{1/2} + 2(\gamma_s^d\gamma_r^d)^{1/2}$, where γ_s and γ_r are the surface energy of the sample and the reference liquid components. The superscripts p and d refer to the polar and dispersion components of the surface energy, respectively. The contact angles of the PVP

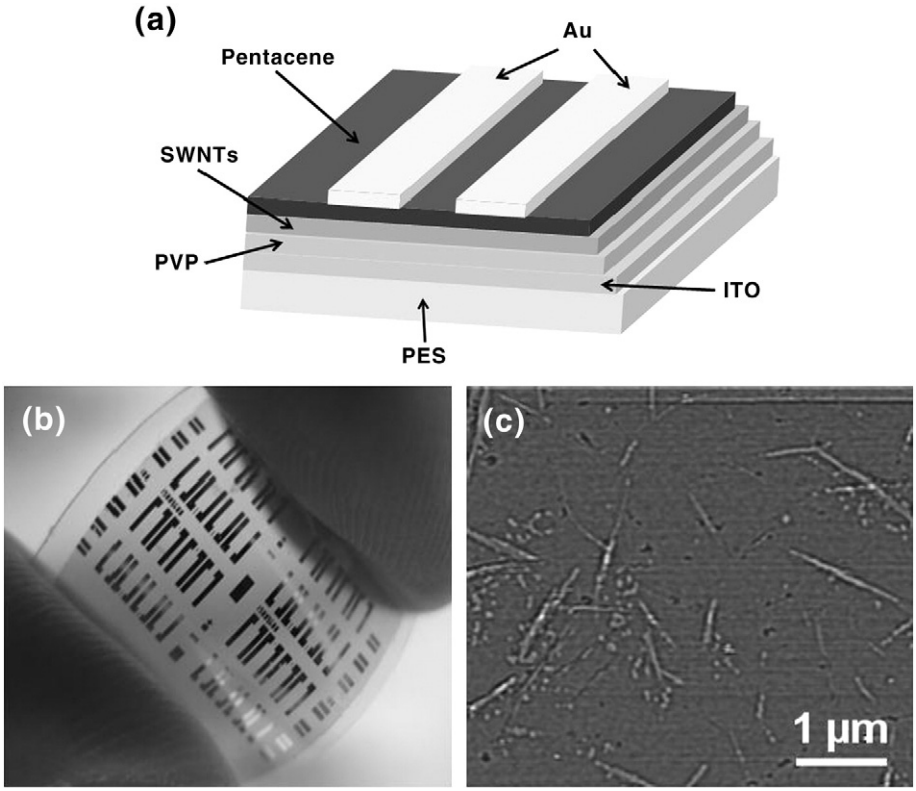

Fig. 1. (a) Schematic of our flexible TFTs with the random SWNTs/pentacene bilayer as active channel, (b) optical image of bended our flexible and semitransparent transistor, and (c) AFM image of the random SWNTs network on PVP dielectric.

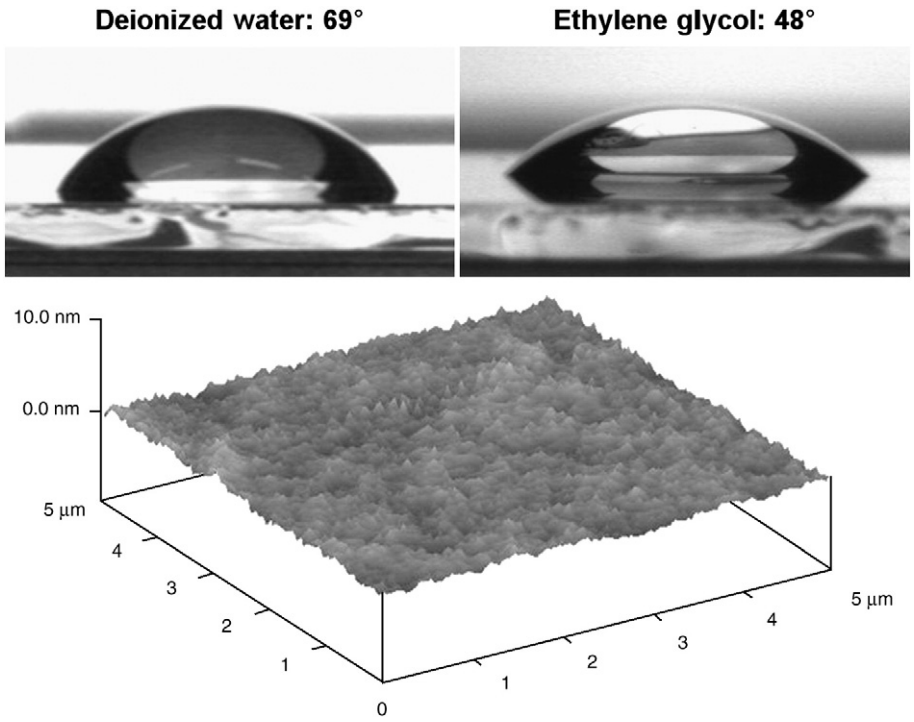

Fig. 2. Atomic force microscopy (AFM) images and contact angles of PVP dielectric.

dielectric were 69° in the deionized water and 48° in the ethylene glycol. This corresponds to a surface energy of 34.4 mJ/m^2. Because SWNTs are hydrophobic, they put down roots well in the non-polar (low surface energy) and smooth surface of the PVP dielectric. In addition, we calculated the capacitance per unit area of the PVP dielectric by $C = \varepsilon_0 \varepsilon_r A/t$, where ε_0 is the free space permittivity, A is the area of the capacitor electrode, and t is the thickness of the dielectric. The dielectric constant of the PVP dielectric was 4.0 at 1 MHz and the capacitance per unit area of the PVP dielectric was 7.9 nF cm^{-2}.

3.2. Morphological and structural properties of pentacene films

The surface morphology and the structural property of the pentacene film were studied with atomic force microscopy (AFM) and X-ray diffraction (XRD) spectroscopy. Fig. 3 shows the XRD spectra and AFM images (inset) of pentacene films that were thermally deposited onto the PVP dielectric and onto the random SWNTs underlay with the PVP dielectric, respectively. From Fig. 3(a), the XRD spectra of the pentacene film that was deposited onto the PVP dielectric had major diffraction peaks that can be attributed to the

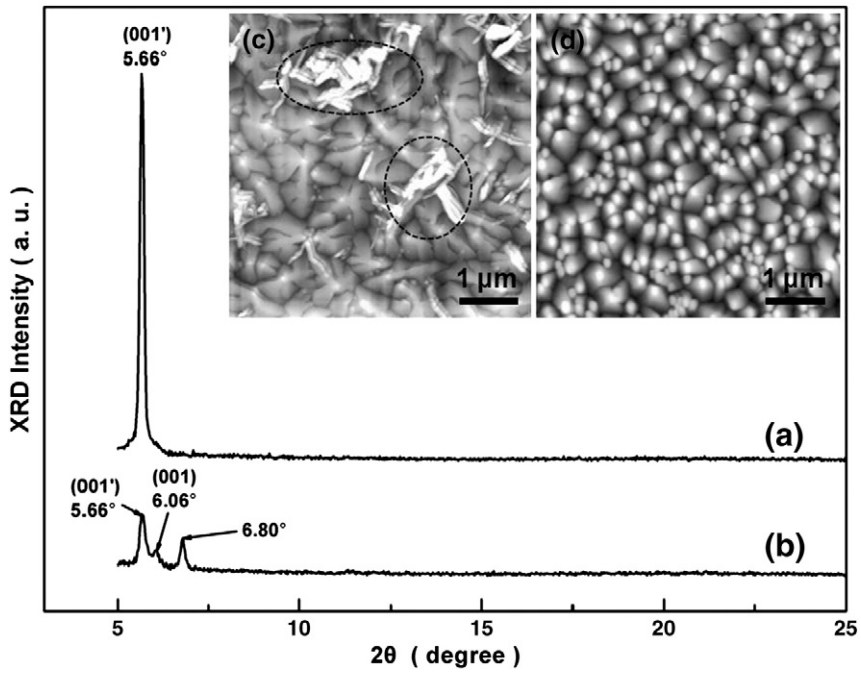

Fig. 3. XRD spectra of 70 nm thick thermally pentacene films deposited onto (a) PVP dielectric and (b) random SWNTs underlay with PVP dielectric. The AFM images in (c) and (d) show the morphologies of pentacene films corresponding to (a) and (b), respectively.

thin-film phase (001′). As shown in Fig. 3(b), the XRD spectra of the pentacene film that was deposited onto the random SWNTs underlay had two major diffraction peaks at 5.66° (thin-film phase) and 6.06° (triclinic bulk phase) that correspond to interlayer separations of 15.6 Å and 14.2 Å, respectively [17]. We observed the same 2θ of the (001′) peak, indicating a well-organized molecular structure with the same layer-by-layer spacing for both pentacene films. Particularly, the sharp peak in the pentacene film that was deposited onto the random SWNTs underlay with the PVP dielectric observed at 6.80° indicates a molecular structure with an interplanar spacing of 12.7 Å, which is nearly consistent with the diameter of SWNTs used in this study. This result shows that the SWNTs underlay has an effect on the molecular growth of crystalline pentacene domains whose nuclei are embedded in an amorphous phase.

The AFM image in Fig. 3(c) shows 'lamellar grains' marked by black dots, in which the molecular growth is inclined in the perpendicular direction [18]. We confirmed that the pentacene film that was deposited on the random SWNTs with the PVP dielectric exhibited a densely grain size and poor crystalline quality (Fig. 3(d)) compared to that with well-formed dendritic grain on the PVP dielectric as judged by the peak intensity of the XRD spectra and the AFM images.

3.3. Electrical performance of OTFTs

We have investigated the effect of the amount of SWNTs on the flexible TFTs performance to establish the optimum concentration of the SWNTs suspension. When the concentration of the SWNTs suspension was higher than 30 mg/l, the mobility of our flexible TFTs was improved but the on/off current ratio became sharply worse, due to the increase in the off-state current (I_{off}). Therefore, we used the SWNTs suspension with a 30 mg/l concentration for the modification layer of the active channel.

Fig. 4 shows the drain current–drain voltage (I_D–V_D) curves obtained from our flexible TFTs fabricated using a single pentacene layer and the SWNTs/pentacene bilayer as an active channel. It can be found that the magnitude of the on-state current (I_{on}) produced by our flexible TFTs with the bilayer was significantly larger than that of the TFTs with a single pentacene layer at the same gate bias (V_G) of −60 V, while having a good saturation characteristic. The electrical characteristics, such as the saturation field effect mobility (μ_{sat}), the threshold voltage (V_{th}), and the on/off current ratio were determined from the $log_{10}(-I_D)-V_G$ and $\sqrt{-I_D}-V_G$ curves of Fig. 5(a) and (b). These are summarized in Table 1. The μ_{sat} of the flexible TFTs with the bilayer was above 2.6×10^{-1} cm^2/Vs. On the other hand, the devices without the SWNTs underlay displayed poor performance with μ_{sat} of 9.7×10^{-2} cm^2/Vs. It was also found that the V_{th} of the flexible TFTs with the bilayer was smaller than that of the flexible TFTs with a single pentacene layer. While our flexible TFTs with the bilayer exhibited a significantly improved behavior in its overall characteristics, the on/off current ratio became slightly worse, due to the increase in I_{off}. As shown in Fig. 1(c), the random SWNTs network had a density of approximately 1 nanotube/μm^2 and an average diameter of 1.2 nm, which corresponds to the band gap energy (E_g)<0.8 eV [19]. The E_g of semiconducting SWNTs is inversely proportional to their diameter, so progressively smaller diameter nanotubes should in fact exhibit larger band gaps [20]. Consequently, the increase in I_{on} is achieved at the expense of a high I_{off} that is caused by a narrow E_g semiconductor and a nominal density metallic component in the random SWNTs underlay. We have debated about the cause of the improvement in μ_{sat}. Generally, grain boundaries in OSC films may act as carrier trap sites, which cause a considerable decrease of the mobility. In our TFTs with the SWNTs underlay in the channel region, carriers could be effectively transported through the SWNTs rod while traversing between the grain boundaries. Moreover, Yoneya et al. have found that the thickness of the effective channel in the TFTs with a pentacene OSC is less than 3 nm from the dielectric surface [21], so we believe that the SWNTs network embedded in the pentacene film offers a channel length reduction effect and a conduction path across the grain boundaries in the dielectric/pentacene interface [10,11].

Although the enhancement of μ_{sat} in flexible TFTs with the SWNTs/pentacene bilayer as an active channel had an inferior result compared with that obtained by other research groups, a dramatic

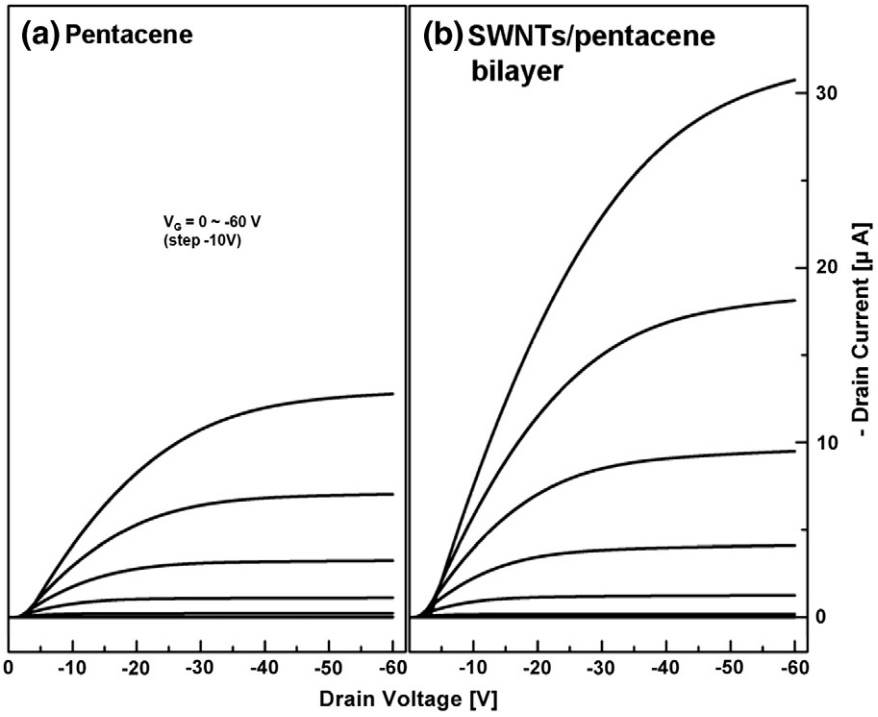

Fig. 4. Drain current–drain voltage (I_D–V_D) curves of our flexible TFTs with (a) the single pentacene layer and (b) the random SWNTs/pentacene bilayer as an active channel. The gate voltage (V_G) ranges from 0 V to −60 V in 10 V steps.

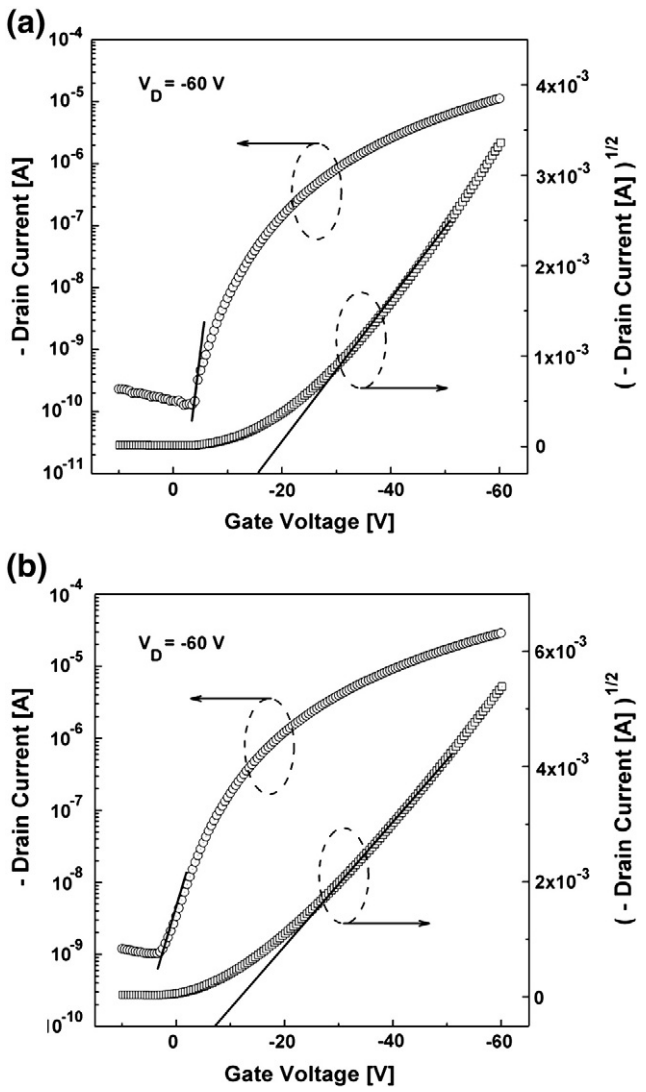

Fig. 5. Current–voltage transfer curves of our flexible TFTs with (a) the single pentacene layer and (b) the random SWNTs /pentacene bilayer as an active channel. $log_{10}(-I_D)-V_G$ curves (circles) show the current on/off ratio and $\sqrt{-I_D}-V_G$ curves (squares) for calculation of saturation field effect mobility that were obtained at drain voltage (V_D) of −60 V.

amelioration in the electrical performance of OTFTs has been based on surface modifications using a self-assembled monolayer (SAM) or a plasma treatment [22–25]. However, the SAM treatment is somewhat disadvantageous because the SAM treatment requires a long immersion time, and the solvent used in the treatment may harm the polymer dielectric and substrate. Also, the plasma treatment needs expensive vacuum equipment. These properties are not compatible with the OTFTs fabrication method that employs the roll-to-roll process technology. Recently, interest has developed in solution-processing OSCs because they may allow low-cost manufacturing approaches. Materials such as poly 3-hexylthiophene (P3HT) and α, ω-dihexylsexithiophene (DH-6 T) are easily deposited, but such OSCs typically have relatively low mobility [26–28]. Because the random SWNTs network is essentially flexible [29], it may enhance the device performance without sacrificing flexibility. Moreover, Artukovic et al. proposed the transparent and flexible TFTs where SWNTs networks having different densities provide both the gate electrode and the active channel [15]. Conclusively, the SWNTs suspension with an optimum concentration for a specific application is compatible with a polymeric substrate for organic electronics based on a simple process and low-cost fabrication, and this is a promising solution for improving inferior electrical performance of the OTFTs.

Table 1
A summary of the electrical characteristics of our flexible TFTs with different active layers.

Active layers	Threshold voltage [V]	Off state current [A]	On state current [A]	On/off current ratio	Mobility [cm^2/Vs]
Pentacene	−15.5	1.3×10^{-10}	1.1×10^{-5}	8.5×10^{4}	9.7×10^{-2}
SWNTs/pentacene	−7	1.0×10^{-9}	2.9×10^{-5}	2.9×10^{4}	2.6×10^{-1}

4. Conclusions

This work demonstrates the solution-processing fabrication and operation of high performance flexible TFTs using a carrier transfer underlay based on a random SWNTs network. We found that a form of the random SWNTs underlay that was produced by a simple coating method prior to pentacene evaporation gave rise to an enhancement in the saturation field effect mobility of our flexible TFTs with a single pentacene layer by a factor 3 with a good on/off current ratio of 10^5. It was also found that the threshold voltage of our flexible TFTs with the bilayer as an active channel was improved compared to that of flexible TFTs with a single pentacene layer. Although the XRD analysis and AFM images show that the pentacene film on the PVP dielectric has a better crystalline quality than that on the random SWNTs underlay with the PVP dielectric, we achieved high performance flexible TFTs using a semiconducting channel and a conduction path offered by the random SWNTs network.

Acknowledgements

This work was supported by the RFID R&D program of MKE/KEIT [10035225, Development of core technology for high performance AMOLED on plastic].

References

[1] S.R. Forrest, Nature 428 (2004) 911.
[2] C.D. Dimitrakopoulos, P.R.L. Malenfant, Adv. Mater. 14 (2002) 99.
[3] A. Sung, M.M. Ling, M.L. Tang, Z. Bao, J. Locklin, Chem. Mater. 19 (2007) 2342.
[4] S.K. Park, J.E. Anthony, D.A. Mourey, T.N. Jacson, Appl. Phys. Lett. 91 (2007) 063514.
[5] J.K. Kim, J.M. Kim, T.S. Yoon, H.H. Lee, D. Jeon, Y.S. Kim, J. Elec. Eng. Technol. 4 (2009) 118.
[6] X.H. Zhang, B. Domercq, X. Wang, S. Yoo, T. Kondo, Z.L. Wang, B. Kippelen, Org. Electron. 8 (2007) 718.
[7] A.P. Graham, G.S. Duesberg, R.V. Seidel, M. Liebau, E. Unger, W. Palmer, F. Kreupl, W. Hoenlein, Small 1 (2005) 382.
[8] A. Javey, J. Guo, Q. Wang, M. Lundstrom, H.J. Dai, Nature 424 (2003) 654.
[9] A. Javey, H. Kim, M. Brink, Q. Wang, A. Ural, J. Guo, P. McIntyre, P. McEuen, M. Lundstrom, H.J. Dai, Nat. Mater. 1 (2002) 241.
[10] X.Z. Bo, C.Y. Lee, M.S. Strano, M. Goldfinger, C. Nuckolls, Graciela B. Blanchet, Appl. Phys. Lett. 86 (2005) 182102.
[11] E.S. Snow, J.P. Novak, P.M. Campbell, D. Park, Appl. Phys. Lett. 82 (2003) 2145.
[12] D.W. Han, J.H. Heo, D.J. Kwak, C.H. Han, Y.M. Sung, J. Elec. Eng. Technol. 4 (2009) 93.
[13] H. Klaul, M. Halik, U. Zschieschang, G. Schmid, W. Radlik, W. Weber, J. Appl. Phys. 92 (2002) 5259.
[14] J.H. Kwon, M.H. Chung, T.Y. Oh, H.S. Bae, J.H. Park, B.K. Ju, F. Yakuphanoglu, Sens. Actuators-A Physical 156 (2009) 312.
[15] E. Artukovic, M. Kaempgen, D.D. Hecht, S. Roth, G. Gruner, Nano Lett. 5 (2005) 757.
[16] J. Kinloch, Adhesion, Champman and Hall, London/New York, 1987 Ch.2.
[17] C.D. Dimitrakopoulos, A.R. Brown, A. Pomp, J. Appl. Phys. 80 (1996) 2501.
[18] H. Yanagisawa, T. Tamaki, M. Nakamura, K. Kudo, Thin Solid Films 398 (2004) 464.
[19] J.W.G. Wildoer, L.C. Venema, A.G. Rinzler, R.E. Smalley, C. Dekker, Nature (London) 391 (1998) 59.
[20] J.W. Mintmire, B.I. Dunlap, C.T. White, Phys. Rev. Lett. 68 (1992) 631.
[21] N. Yoneya, M. Noda, N. Hirai, K. Nomoto, Appl. Phys. Lett. 85 (2004) 4663.
[22] M. Shtein, J. Mapel, J.B. Benziger, S.R. Forrest, Appl. Phys. Lett. 81 (2002) 268.
[23] D. Knipp, R.A. Street, A. Völkel, J. Ho, J. Appl. Phys. 93 (2003) 347.
[24] S.C. Lim, J.H. Lee, M.K. Kim, D.J. Kim, T. Zyung, S.H. Kim, Synth. Met. 148 (2005) 75.

[25] C.S. Kim, S.J. Jo, J.B. Kim, S.Y. Ryu, J.H. Noh, S.J. Lee, Y.S. Kim, H.K. Baik, Appl. Phys. Lett. 91 (2007) 063503.
[26] D.H. Kim, Y.D. Park, Y. Jang, H. Yang, Y.H. Kim, J.I. Han, D.G. Moon, S. Park, T. Chang, M. Joo, C.Y. Ryu, K. Cho, Adv. Funct. Mater. 15 (2005) 77.
[27] J.H. Kown, J.H. Seo, H. Kang, D.H. Choi, B.K. Ju, J. Appl. Phys. 101 (2007) 064502.
[28] H. Kang, K.K. Han, J.E. Park, H.H. Lee, Org. Electron. 8 (2007) 460.
[29] N. Saran, K. Parikh, D.S. Suh, E. Munoz, H. Kolla, S.K. Manohar, J. Am. Chem. Soc. 126 (2004) 4462.